Transport-Equilibrium Schemes for Pedestrian Flows with Nonclassical Shocks

Christophe Chalons

Université Paris 7 - Denis Diderot & Laboratoire J.-L Lions, U.M.R. 7598, Université Pierre et Marie Curie, Boîte courrier 187, 75252 Paris Cedex 05, France.
E-mail: chalons@math.jussieu.fr

Abstract. This paper deals with the numerical approximation of the solutions of a macroscopic model for the description of the flow of pedestrians. Solutions of the associated Riemann problem are known to be possibly *nonclassical* in the sense that the underlying discontinuities may well violate Oleinik inequalities, which makes very sensitive their numerical approximation. This study proposes to apply to this framework the Transport-Equilibrium strategy proposed in [2] for computing nonclassical solutions of scalar conservation laws. Numerical evidences are proposed.

1 Introduction

In this paper, we are interested in the numerical approximation of weak solutions of a scalar conservation law arising in the description of the flow of pedestrians. The model under consideration has been introduced recently by Colombo and Rosini in [8]. It is based on the well-known Lighthill-Whitam [14] and Richards [15] model and writes

$$\begin{cases} \partial_t \rho + \partial_x q(\rho) = 0, \;\; \rho(x,t) \in \mathbb{R}, \;\; (x,t) \in \mathbb{R} \times \mathbb{R}^{+*}, \\ \rho(x,0) = \rho_0(x), \;\; x \in \mathbb{R}, \end{cases} \tag{1}$$

where $\rho \geq 0$ is the pedestrian density and $q : \mathbb{R}^+ \to \mathbb{R}^+$ is the flow function. The form of equation (1) is an immediate consequence of two basic assumptions, namely the conservation of the total number of pedestrians and a given speed law v which depends on density $\rho \in [0, R]$ only (R denotes the maximal density). Recall that $q = \rho v$. However, this model was first dedicated to car flows and so is not able to reproduce important features of pedestrian flows, at least when considering typical concave increasing - decreasing flow functions. For instance let us mention the *overcompression phenomenon* in a crowd or the *fall of pedestrians* in the outflow through a door of a crowd in panic. In order to overcome this difficulty, Colombo and Rosini [8] first proposed to modify the typical shape of the flow function q by introducing another characteristic density $R^\star > R$ for the maximal density in exceptional situations of panic. The flow function now looks like a concave - convex and increasing - decreasing function on $[0, R]$ and a convex - concave and increasing - decreasing function on $[R, R^\star]$. See Figure 1 below. In particular, discontinuities satisfying the usual Rankine-Hugoniot conditions but violating the standard admissibility entropic conditions such as

Oleinik inequalities (see (6) below) are present in the model. Then, the same authors defined a unique Riemann solver using such nonclassical shocks. The main motivation in considering nonclassical solutions is to allow panic states ($\rho \in [R, R^\star]$) to appear in a initially calm situation ($\rho \in [0, R]$), because of a sharp increase in the density for instance. Note that the *maximum principle* in classical solutions prevents such panic situations from arising. We refer the reader to [12] for a general theory of classical and nonclassical solutions.
From a numerical point of view, the numerical approximation of nonclassical solutions is known to be very challenging and still constitutes (at least generally speaking) an open problem nowadays (see for instance [9], [10], [13], [4], [5], [6], but also [1] and the references within). Very recently, a new efficient numerical strategy has been proposed in [2] for computing nonclassical solutions of scalar conservation laws. Roughly speaking, the corresponding finite volume scheme is based on two steps, namely an *Equilibrium step* of which aim is to put at stationary equilibrium nonclassical discontinuities when present, and a *Transport step* for propagating these discontinuities. In this paper, we thus propose to adapt the Transport-Equilibrium scheme developed in [2] to the present setting. We refer the reader to [3] for details about the slight (but important) difference between both algorithms. Importantly, we will see that the resulting scheme still provides numerical solutions in full agreement with exact ones.

2 Governing Equation and Closure Relation

The model we consider for the description of the flow of pedestrians has been recently introduced and studied by Colombo and Rosini [8]. It is based on the well-known Lighthill-Whitam [14] and Richards [15] model and writes as

$$\begin{cases} \partial_t \rho + \partial_x q(\rho) = 0, \quad q(\rho) = \rho v(\rho), \ \ (x,t) \in \mathbb{R} \times \mathbb{R}^{+*}, \\ \rho(x,0) = \rho_0(x), \ \ x \in \mathbb{R}, \end{cases} \tag{2}$$

where ρ is the pedestrian density, q is the flux function and v the speed of pedestrians. For simplicity, initial data ρ_0 is assumed to be made of two constant states ρ_l and ρ_r, separated by a discontinuity located at point $x = 0$:

$$\rho_0(x) = \begin{cases} \rho_l \text{ if } x < 0, \\ \rho_r \text{ if } x > 0. \end{cases} \tag{3}$$

Equation (2) expresses the conservation of the number of pedestrians in the space domain, while the speed v is assumed to depend only on the density ρ by means of the so-called *fundamental relation*. In the context of car flows, it is pretty classical to consider that the function $\rho \in [0, R] \to q(\rho)$ is concave, with $q(0) = q(R) = 0$, R being the maximal density, and reaches its maximum value at a critical density $R_M \in [0, R] : q(R_M) = \max_{\rho \in [0,R]} q(\rho)$. Here and in order to take into account some important features of human flows, like the *overcompression phenomenon* or the *fall of pedestrians* due to panic for instance, we follow [8] and take a flux function q whose form is given on Figure 1. Two

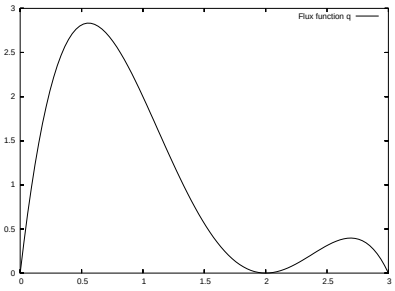

Fig. 1. Closure relations : $\rho \to q(\rho)$

remarkable values R and $R^\star$ ($R < R^\star$) are now considered for the density ρ : the first one represents a natural bound of ρ in situations with little or not panic ($\rho \in [0, R]$), and the second one is a maximal value of ρ in situations of great panic ($\rho \in [R, R^\star]$). The flow function q now admits in each of these regions a maximum value : $R_M \in [0, R]$ with $q(R_M) = \max_{\rho\in[0,R]} q(\rho)$ and $R_M^\star \in [R, R^\star]$ with $q(R_M^\star) = \max_{\rho\in[R,R^\star]} q(\rho)$ as well as an inflection point : $R_I \in [0, R]$ with $q''(R_I) = 0$ and $R_I^\star \in [R, R^\star]$ with $q''(R_I^\star) = 0$, while $q(0) = q(R) = q(R^\star) = 0$. Choosing (without loss of generality in the forthcoming developments)

$$q(\rho) = -\rho(\rho - R)^2(\rho - R^\star), \quad R = 2, \quad R^\star = 3, \tag{4}$$

the following values are easily found :

$$R_M \simeq 0.5570, \quad R_M^\star \simeq 2.6930, \quad R_I \simeq 1.1208, \quad R_I^\star \simeq 2.3792. \tag{5}$$

3 The Riemann Solver

Let us now turn to the definition of a Riemann solution for (2)-(3)-(4). First of all, let us recall that there exists a unique *classical* solution for (2)-(3)-(4), that is a weak solution selected by the validity of Oleinik inequalities across discontinuities separating ρ_- and ρ_+ :

$$\frac{q(\rho) - q(\rho_-)}{\rho - \rho_-} \geq \frac{q(\rho_+) - q(\rho_-)}{\rho_+ - \rho_-}, \text{ for all } \rho \text{ between } \rho_- \text{ and } \rho_+. \tag{6}$$

Moreover, this solution obeys the following maximum principle property

$$\rho(x,t) \in [\min(\rho_l, \rho_r), \max(\rho_l, \rho_r)], \quad \text{for all} \quad x \in \mathbb{R} \quad \text{and} \quad t \geq 0. \tag{7}$$

See for instance [12] for details. In this context, imagine that ρ_l and ρ_r belong to the calm region $[0, R]$. Then, due to the maximum principle (7), no panic state may be found in the *classical* solution. From a practical point of view, such a panic state is nevertheless expected to appear in certain situations when ρ_r is very close to R. That is the reason for which *nonclassical* solutions violating both

the maximum principle property and Oleinik inequalities across discontinuities are introduced in the present framework. With this in mind and following [8] and [12], we define two functions $\psi : [0, R^\star] \to [R, R^\star]$ and $\Phi : [0, R] \to [0, R]$, related to the graph of function q in the (ρ, q)-plane, as follows :

- $\psi(\rho)$ is such that the line L_ρ that passes through the points with coordinates $(\rho, q(\rho))$ and $(\psi(\rho), q(\psi(\rho)))$ is tangent to the graph of function q at point $(\psi(\rho), q(\psi(\rho)))$

- $\Phi(\rho)$ is such that this line intersects the curve $q = q(\rho)$ at a further point with coordinates $(\Phi(\rho), q(\Phi(\rho)))$

An illustration is given on Figure 2 - Left where both the function q and the line $L_{\rho=0.5}$ are plotted. The right part of Figure 2 is concerned with the graph of both functions ψ and Φ. In particular, note that Φ is not defined in the whole domain $[0, R]$ simply because the additional intersection point between L_ρ and q is sometimes realized below 0.

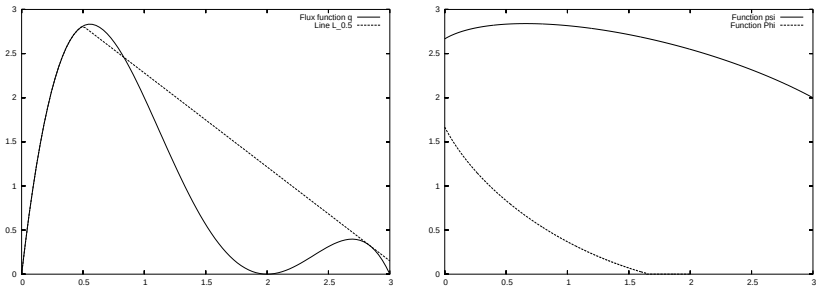

Fig. 2. Function q and line $L_{0.5}$ (Left) - Functions ψ and Φ (Right)

Then, introducing s and Δs be two real thresholds such that

$$s \in]0, R_M[\quad \text{and} \quad \Delta s \in]0, R - s[, \tag{8}$$

Colombo and Rosini [8] defined a unique Riemann solution for (2)-(3)-(4), which coincides with the *classical* solution except in the next three situations :
(i) (ρ_l, ρ_r) belongs to A with

$$A = \{(\rho_l, \rho_r) \in [0, R^\star]^2 \ / \ s \leq \rho_l \leq R, \ \Phi(\rho_l) < \rho_r \leq R, \ (\rho_r - \rho_l) > \Delta s\}, \tag{9}$$

(ii) (ρ_l, ρ_r) belongs to B with

$$B = \{(\rho_l, \rho_r) \in [0, R^\star]^2 \ / \ \rho_r > R, \ \rho_r > \rho_l, \ \rho_r \leq \psi(\rho_l)\}, \tag{10}$$

(iii) (ρ_l, ρ_r) belongs to C with

$$C = \{(\rho_l, \rho_r) \in [0, R^\star]^2 \ / \ \rho_r > R, \ \rho_r > \rho_l, \ \rho_r > \psi(\rho_l)\}. \tag{11}$$

The last two situations aim at defining the solution when the right state ρ_r belongs to the panic area, *i.e.* $\rho_r > R$. More precisely, if ρ_l and ρ_r are such

that (ρ_l, ρ_r) belongs to B the Riemann solution contains a nonclassical shock connecting ρ_l to $\psi(\rho_l)$ followed by the classical Riemann solution associated with initial states $\psi(\rho_l)$ and ρ_r. And if ρ_l and ρ_r are such that (ρ_l, ρ_r) belongs to C, the Riemann solution is a nonclassical shock connecting ρ_l to ρ_r. In this paper, we will focus (without restriction) on the first situation $(\rho_l, \rho_r) \in A$ which explains that if the left state ρ_l is sufficiently large ($\rho_l \geq s$) and faces a right state ρ_r which is pretty far ($\rho_r - \rho_l > \Delta s$) from ρ_l and already close to the panic region ($\Phi(\rho_l) < \rho_r \leq R$), then a panic state is created due to the sharp increase in the density. So that the maximum principle property is violated, and the corresponding solution is made of a nonclassical shock connecting ρ_l to $\psi(\rho_l)$ followed by the classical Riemann solution associated with initial states $\psi(\rho_l)$ and ρ_r.
Before addressing the numerical approximation of these Riemann solutions, it is worth noticing that function ψ plays the part of a *kinetic function* that manages the transitions between calm and panic. Finally, we refer the reader to [8] for additional properties of interest satisfied (or not) by the Riemann solver proposed in this section.

4 Numerical Approximation

Aim of this section is the description of the so-called Transport-Equilibrium schemes recently proposed by the author for approximating nonclassical solutions of conservation laws. The work proposed in [2] is concerned with scalar conservation laws, while the case of systems will be treated in a subsequent paper. Applying these schemes to the model of pedestrian flows under consideration is the main objective of this section. We begin by introducing some notations.
Let Δt and Δx be the time and the space steps. Introducing the interfaces $x_{j+1/2} = j\Delta x$ for $j \in \mathbb{Z}$ and the intermediate times $t^n = n\Delta t$ for $n \in \mathbb{N}$, we classicaly seek at each time t^n an approximation ρ_j^n of solution $x \to \rho(x, t^n)$ on each interval $C_j = [x_{j-1/2}; x_{j+1/2}),\ j \in \mathbb{Z}$. In this context, we assume as given a two-point (without loss of generality) numerical flux function $(u, v) \to g(u, v)$ consistent with the flux fonction q, and we set $\lambda = \Delta t/\Delta x$.

In order to motivate the need of a particular treatment when numerically dealing with nonclassical solutions, let us have a look on what happens when considering the following classical conservative scheme :

$$\rho_j^{n+1} = \rho_j^n - \lambda(g_{j+1/2} - g_{j-1/2}), \quad j \in \mathbb{Z}, \tag{12}$$

with $g_{j+1/2} = g(\rho_j^n, \rho_{j+1}^n)$ for all $j \in \mathbb{Z}$. Figure 3 - Left shows the solution generated by a standard Relaxation numerical flux g (see (19) below) when initial states ρ_l and ρ_r are such that $(\rho_l, \rho_r) \in A$. In other words, the exact solution contains a transition between calm and panic regions that should be observed via a *nonclassical* shock connecting ρ_l to $\psi(\rho_l)$. On the contrary, we note that the numerical solution is *classical* and then remains entirely calm. Which means that update formula (12) is not able to create by itself the panic

state $\psi(\rho_l)$. The same failure would be observed with $(\rho_l, \rho_r) \in B$. *Then, one must enforce the appearance of the corresponding discontinuity between* ρ_l *and* $\psi(\rho_l)$ *when it is relevant, that is when* $(\rho_l, \rho_r) \in A$ *and when* $(\rho_l, \rho_r) \in B$.

Actually, it turns out that the conservative scheme (12) is not either able to

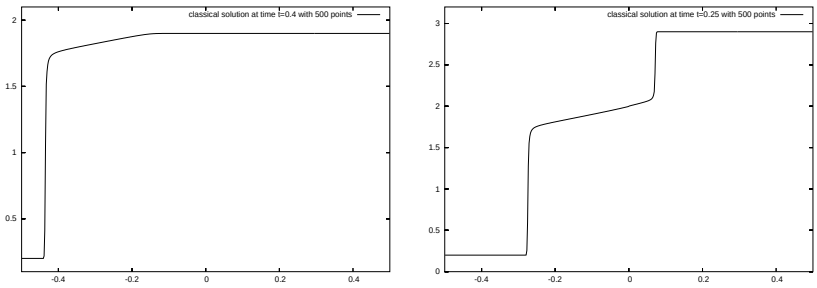

Fig. 3. Solution generated by standard Relaxation method when $(\rho_l, \rho_r) \in A$ (Left) and $(\rho_l, \rho_r) \in C$ (Right)

properly capture the exact *nonclassical* solution when $(\rho_l, \rho_r) \in C$, that is in the case when the Riemann initial data (3) should be simply propagated at speed $\sigma(\rho_l, \rho_r)$ given by Rankine-Hugoniot jump relation :

$$\sigma(\rho_l, \rho_r) = \frac{q(\rho_r) - q(\rho_l)}{\rho_r - \rho_l}. \tag{13}$$

Instead, a classical solution is observed on Figure 3 - Right. *Then, one must enforce the initial data to be simply propagated (at the right speed !) when it is relevant, that is when* $(\rho_l, \rho_r) \in C$.

These observations led us to replace (12) with the following nonconservative update formula :

$$\rho_j^{n+1-} = \rho_j^n - \lambda(g_{j+1/2}^L - g_{j-1/2}^R), \quad j \in \mathbb{Z}, \tag{14}$$

where the numerical fluxes $g_{j+1/2}^L$ and $g_{j+1/2}^R$ have to be suitably defined. The very idea is to modify the numerical flux $g_{j+1/2}$ by means of two fluxes $g_{j+1/2}^L$ and $g_{j+1/2}^R$ each time that a nonclassical shock appears in the solution of the Riemann problem (2)-(3)-(4) associated with $\rho_l = \rho_j^n$ and $\rho_r = \rho_{j+1}^n$. Otherwise, $g_{j+1/2}$ will be unchanged. According to whether the nonclassical shock connects states ρ_l and $\psi(\rho_l)$ or not, that is depending on if $(\rho_j^n, \rho_{j+1}^n) \in A \cup B$ or $(\rho_j^n, \rho_{j+1}^n) \in C$, we will use different formulas. More precisely, we set for all $j \in \mathbb{Z}$:

$$g_{j+1/2}^L = \begin{cases} g(\rho_j^n, \rho_j^n) & \text{if} \quad (\rho_j^n, \rho_{j+1}^n) \in A \cup B \cup C, \\ g(\rho_j^n, \rho_{j+1}^n) & \text{otherwise,} \end{cases} \tag{15}$$

and

$$g^R_{j+1/2} = \begin{cases} g(\psi(\rho^n_j), \rho^n_{j+1}) & \text{if} \quad (\rho^n_j, \rho^n_{j+1}) \in A \cup B, \\ g(\rho^n_{j+1}, \rho^n_{j+1}) & \text{if} \quad (\rho^n_j, \rho^n_{j+1}) \in C, \\ g(\rho^n_j, \rho^n_{j+1}) & \text{otherwise.} \end{cases} \tag{16}$$

The aim of $g^L_{j+1/2}$ is to keep at the next time step the same value ρ^n_j in the cell C_j since ρ^n_j always coincides with the left state of the nonclassical shock in the Riemann solution associated with $\rho_l = \rho^n_j$ and $\rho_r = \rho^n_{j+1}$. The aim of $g^R_{j+1/2}$ is double. First, to keep the same value ρ^n_{j+1} in the cell C_{j+1} when $(\rho^n_j, \rho^n_{j+1}) \in C$, since ρ^n_{j+1} coincides in this case with the right state of the nonclassical shock in the Riemann solution associated with $\rho_l = \rho^n_j$ and $\rho_r = \rho^n_{j+1}$. And then, to force the value $\psi(\rho^n_j)$ to appear in the cell C_{j+1} when $(\rho^n_j, \rho^n_{j+1}) \in A \cup B$.

With these definitions, we easily check for instance that discontinuities separating two states ρ_- and ρ_+ such that $(\rho_-, \rho_+) \in C$ are kept at stationary equilibrium by formulas (14)-(15)-(16). See also [2] or [3] for more details. More generally, we are thus bound to introduce a dynamic step in order to make moving the values that we previously forced to be present in specific cells.
Recall that the speed of propagation $\sigma(\rho_-, \rho_+)$ of a discontinuity between ρ_- and ρ_+ is given by Rankine-Hugoniot conditions (13). We then decide to define at each interface $x_{j+1/2}$ a speed of propagation $\sigma_{j+1/2}$:

$$\sigma_{j+1/2} = \begin{cases} \sigma(\rho^{n+1-}_j, \rho^{n+1-}_{j+1}) & \text{if} \quad (\rho^n_j, \rho^n_{j+1}) \in A \cup B \cup C, \\ 0 & \text{otherwise,} \end{cases} \tag{17}$$

and solve locally (at each discontinuity $x_{j+1/2}$) a transport equation with speed $\sigma_{j+1/2}$. In order to get a new approximation ρ^{n+1}_j at time $t^{n+1} = t^n + \Delta t$, we propose to pick up randomly on interval $[x_{j-1/2}, x_{j+1/2}[$ a value in the juxtaposition of the solutions of these transport equations at time Δt that we choose sufficiently small to avoid wave interactions. In particular, such a sampling strategy prevents the emergence of spurious intermediate values with respect to those obtained at time t^{n+1-}. See again [2] or [3] for more details. Given a well distributed random sequence (a_n) within interval $(0, 1)$, it amounts to set :

$$\rho^{n+1}_j = \begin{cases} \rho^{n+1-}_{j-1} \text{ if } a_{n+1} \in [0, \lambda\sigma^+_{j-1/2}[, \\ \rho^{n+1-}_j \text{ if } a_{n+1} \in [\lambda\sigma^+_{j-1/2}, 1 + \lambda\sigma^-_{j+1/2}[, \\ \rho^{n+1-}_{j+1} \text{ if } a_{n+1} \in [1 + \lambda\sigma^-_{j+1/2}, 1[, \end{cases} \tag{18}$$

with $\sigma^+_{j+1/2} = \max(\sigma_{j+1/2}, 0)$ and $\sigma^-_{j+1/2} = \min(\sigma_{j+1/2}, 0)$ for all $j \in \mathbb{Z}$. The description of our numerical strategy is now completed.

5 Numerical Experiments

This section proves the good design of the transport-equilibrium scheme we have proposed. To that purpose and without restriction, we consider a Relaxation

scheme as a basic numerical flux g, that is

$$g(u,v) = \frac{1}{2}(q(u)+q(v)) + \frac{a(u,v)}{2}(u-v) \quad \text{with} \quad a(u,v) = \max_{[\min(u,v),\max(u,v)]} |q'|, \tag{19}$$

(see [11] for instance) and we use the following standard CFL condition for computing time step Δt at each time iteration :

$$\Delta t = \frac{1}{2} \times \frac{\Delta x}{\max_j |a(\rho_j^n, \rho_{j+1}^n)|}.$$

Following a proposal by Collela [7], we consider the van der Corput random sequence (a_n) defined by

$$a_n = \sum_{k=0}^{m} i_k 2^{-(k+1)},$$

where $n = \sum_{k=0}^{m} i_k 2^k$, $i_k = 0, 1$, denotes the binary expansion of the integers $n = 1, 2, ...$ Closure relations for the numerical simulations are as follows. First of all, the flux function q is chosen as in (4) (see also (5) and Figure 1 for the graph of function q). Then, thresholds s and Δs are chosen to be

$$\Delta s = \Phi(0) = \frac{5}{3}, \quad s = \frac{1}{2}(R - \Delta s) = \frac{1}{6},$$

so that condition (8) holds true. As last, we mention that the computations are performed on two grids, containing respectively 100 ($\Delta x = 0.01$) and 500 ($\Delta x = 0.002$) points per unit interval. Let us now consider two typical behaviors of the Riemann solution given in Section 3. We refer the reader to [3] for additional numerical tests.

In Test 1, we choose $\rho_l = 0.2$ and $\rho_r = 1.9$ so that it is easily checked that $(\rho_l, \rho_r) \in [0, R]^2$ and $(\rho_l, \rho_r) \in A$. In such a situation, panic arises and the solution is composed of a nonclassical discontinuity between $\rho_l = 0.2$ and $\psi(\rho_l) \simeq 2.7744$, followed by a classical part made of a rarefaction wave and a classical shock attached to the rarefaction. We observe on Figure 4 - Left that our algorithm properly captures this nonclassical solution. Note also that the nonclassical discontinuity from ρ_l to $\psi(\rho_l)$ is sharp : there is no point in the profile. For the sake of comparison, Figure 4 - Right shows again that the usual Relaxation scheme defined by update formula (12) generates a (classical) solution which lies entirely in interval $[0, R]$ and so is far from the expected one. What proves both the need of modifying classical conservative approaches and the validity of our strategy.

In Test 2, we take $\rho_l = 0.2$ and $\rho_r = 2.9$ so that we have now $(\rho_l, \rho_r) \in C$. By Section 3, the solution is a single nonclassical shock connecting ρ_l to ρ_r. Figure 5 - Left shows that our algorithm again sharply captures this nonclassical discontinuity. Actually, note that it and Glimm's random choice scheme are identical for this test case since the equilibrium step is clearly transparent. The solution obtained with the standard Relaxation scheme is plotted again on Figure 5 - Right.

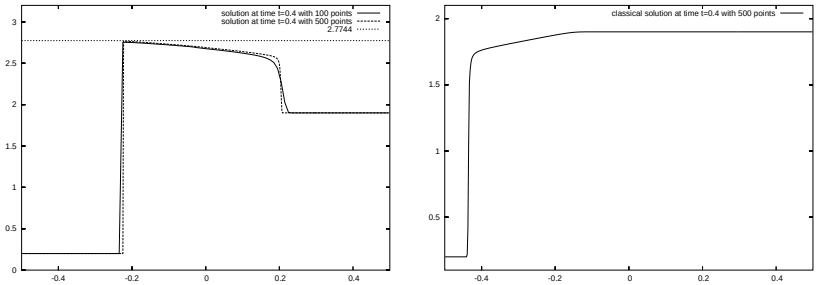

Fig. 4. Test 2 - nonclassical solution (Left) and classical solution (Right)

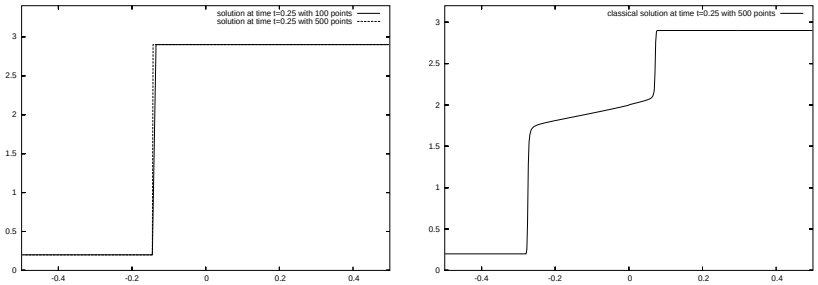

Fig. 5. Test 5 - nonclassical solution (Left) and classical solution (Right)

6 Conclusion

An efficient numerical strategy has been presented for computing nonclassical solutions of a particular scalar conservation law for the simulation of human flows. Our approach turns out to be nonconservative, but measures in [3] have shown that the loss of mass is extremely low, while numerical solutions fully agree with exact ones.

References

1. Chalons C., *Bilans d'entropie discrets dans l'approximation numérique des chocs non classiques. Application aux équations de Navier-Stokes multi-pression 2D et à quelques systèmes visco-capillaires*, PhD Thesis, Ecole Polytechnique, (2002).
2. Chalons C., *Transport-Equilibrium Schemes for Computing Nonclassical Shocks. I. Scalar Conservation Laws*, Preprint of the Laboratoire Jacques-Louis Lions (2005).
3. Chalons C., *Numerical approximation of a macroscopic model of pedestrian flows*, Preprint of the Laboratoire Jacques-Louis Lions (2005).
4. Chalons C. et LeFloch P.G., *A fully discrete scheme for diffusive-dispersive conservation laws*, Numerisch Math., vol 89, pp 493-509 (2001).
5. Chalons C. et LeFloch P.G., *High-order entropy conservative schemes and kinetic relations for van der Waals fluids*, J. Comput. Phys., vol 167, pp 1-23 (2001).

6. Chalons C. and LeFloch P.G., *Computing undercompressive waves with the random choice scheme. Nonclassical shock waves*, Interfaces and Free Boundaries, vol 5, pp 129-158 (2003).
7. Collela P., *Glimm's method for gas dynamics*, SIAM J. Sci. Stat. Comput., vol 3, pp 76-110 (1982).
8. Colombo R.M. and Rosini M.D., *Pedestrian Flows and Nonclassical Shocks*, Mathematical Methods in the Applied Sciences, vol 28, issue 13, pp 1553-1567 (2005).
9. Hayes B.T. and LeFloch P.G., *Nonclassical shocks and kinetic relations : Scalar conservation laws*, Arch. Rational Mech. Anal., vol 139, pp 1-56 (1997).
10. Hayes B.T. and LeFloch P.G., *Nonclassical shocks and kinetic relations : Finite difference schemes*, SIAM J. Numer. Anal., vol 35, pp 2169-2194 (1998).
11. Lattanzio C. and Serre D., *Convergence of a relaxation scheme for hyperbolic systems of conservation laws*, Numer. Math., vol 88, pp 121-134 (2001).
12. LeFloch P.G., **Hyperbolic Systems of Conservation Laws: The theory of classical and nonclassical shock waves**, E.T.H. Lecture Notes Series, Birkhäuser (2002).
13. LeFloch P.G. and Rohde C., *High-order schemes, entropy inequalities, and nonclassical shocks*, SIAM J. Numer. Anal., vol 37, pp 2023-2060 (2000).
14. Lighthill M.J. and Whitham G.B., *On kinematic waves. II. A theory of traffic flow on long crowded roads*, Proc. Royal Soc. London, Ser. A., vol 229, pp 317-345 (1955).
15. Richards P.I., *Shock waves on the highway*, Operations Res., vol 4, pp 42-51 (1956).